JACS
JOURNAL OF THE AMERICAN CHEMICAL SOCIETY

Communication

pubs.acs.org/JACS

Quantum Switching of π-Electron Rotations in a Nonplanar Chiral Molecule by Using Linearly Polarized UV Laser Pulses

Hirobumi Mineo,[†] Masahiro Yamaki,[§] Yoshiaki Teranishi,[∥] Michitoshi Hayashi,[‡] Sheng Hsien Lin,[§,⊥] and Yuichi Fujimura*[,§,⊥,#]

[†]Institute of Applied Mechanics and [‡]Center for Condensed Matter Science, National Taiwan University, Taipei 106, Taiwan

[§]Department of Applied Chemistry, Institute of Molecular Science, and [∥]Institute of Physics, National Chiao-Tung University, Hsin-Chu 300, Taiwan

[⊥]Institute of Atomic and Molecular Sciences, Academia Sinica, Taipei 106, Taiwan

[#]Department of Chemistry, Graduate School of Science, Tohoku University, Sendai 980-8578, Japan

S *Supporting Information*

ABSTRACT: Nonplanar chiral aromatic molecules are candidates for use as building blocks of multidimensional switching devices because the π electrons can generate ring currents with a variety of directions. We employed (*P*)-2,2′-biphenol because four patterns of π-electron rotations along the two phenol rings are possible and theoretically determine how quantum switching of the π-electron rotations can be realized. We found that each rotational pattern can be driven by a coherent excitation of two electronic states under two conditions: one is the symmetry of the electronic states and the other is their relative phase. On the basis of the results of quantum dynamics simulations, we propose a quantum control method for sequential switching among the four rotational patterns that can be performed by using ultrashort overlapped pump and dump pulses with properly selected relative phases and photon polarization directions. The results serve as a theoretical basis for the design of confined ultrafast switching of ring currents of nonplanar molecules and further current-induced magnetic fluxes of more sophisticated systems.

Laser control of electrons in molecular systems has attracted considerable attention because the generated currents can be new sources of next-generation ultrafast switching devices.[1−4] In particular, π electrons in aromatic molecules have potential usefulness for organic nanoelectronics and optoelectronics.[5,6] In addition, they are the origin of aromaticity, which is an essential concept of conjugated molecules.[7,8] Recently there have been several theoretical studies of the generation and control of π-electron motions in molecular systems using ultrashort UV pulsed lasers. Manz's group has shown by quantum-chemical simulations that the π electrons of Mg porphyrin can be rotated along the aromatic ring by using circularly polarized UV laser pulses.[9] The direction of the π-electron rotation, clockwise or anticlockwise, can be determined by applying right or left circularly polarized laser pulses. Kanno and co-workers have proposed the use of linearly polarized UV laser pulses to create π-electron rotations along the ring of 2,5-dichloro[*n*](3,6)pyrazinophane.[10] This molecule is one of the chiral molecules with planar chirality. The aromatic ring, pyrazine, has no degenerate electronic states that create electronic angular momentum. In this case, the electronic angular momentum can be generated by coherent excitation of a pair of two quasi-degenerate excited states.

In the *planar* aromatic molecules reported in refs 9 and 10, π electrons create electronic angular momentum perpendicular to their aromatic ring; that is, the electronic ring current is only within the molecular plane. *Nonplanar* aromatic ring molecules, on the other hand, are promising candidates for use in sophisticated switching devices with several controllable variables because of their multidimensional angular momenta created by π-electron motions. Each π-electron rotation has a particular angular momentum vector with a definite direction and generates the corresponding electron current.

In this work, we used (*P*)-2,2′-biphenol, which is a typical nonplanar chiral aromatic molecule with axial chirality.[11] The rotational dynamics of π electrons in chiral molecules with a single aromatic ring has been elucidated.[10] On the other hand, no guiding principle for controlling π-electron rotations in nonplanar aromatic molecules has been reported. For π electrons in 2,2′-biphenol, there are four possible rotational patterns: CC, AA, CA, and AC, where C and A refer to clockwise and anticlockwise rotation and the first and second letters in each pattern refer to the left (L) and right (R) phenol rings, respectively (see Figure 2a below). In this investigation, we first clarified how these patterns can be prepared and then how ultrafast switching between these rotational patterns can be realized.

The geometry of (*P*)-2,2′-biphenol in the ground state was optimized using density functional theory (DFT) at the B3LYP level as implemented in the Gaussian 09 program.[12] The energies of the electronic excited states were calculated at the optimized ground-state geometry using time-dependent DFT (TDDFT) at the B3LYP level [see the Supporting Information (SI)]. The 6-31G+(d,p) basis set was used throughout our calculations.[13] The dihedral angle between the two phenol groups was found to be 108.8° from our DFT calculations.

Received: May 17, 2012

   dx.doi.org/10.1021/ja3047848 | *J. Am. Chem. Soc.* XXXX, XXX, XXX−XXX

For preparation of the four patterns of π-electron rotations, we focused on the three optically allowed excited states whose energies range from 6.67 to 6.84 eV (Figure 1a). The lowest of

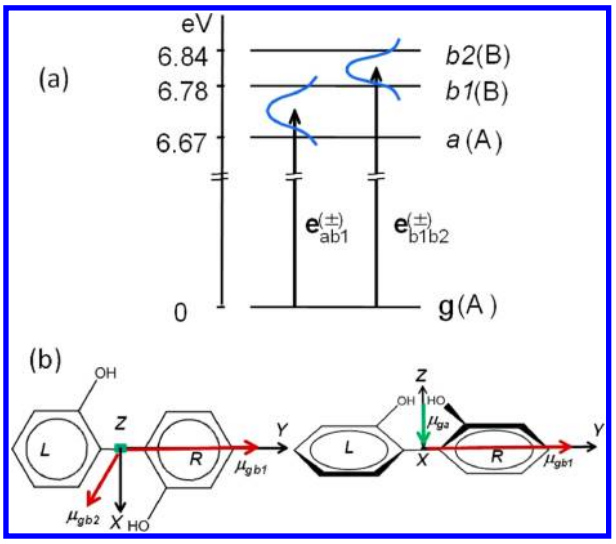

Figure 1. (a) Three electronic excited states (a, b_1, and b_2) of (*P*)-2,2′-biphenol and coherent excitations of two excited states. (b) Transition dipole moments between the ground and excited states.

these three excited state, with an excitation energy of 6.67 eV, belongs to the totally symmetric irreducible representation A in the C_2 point group and is denoted by a. The other two excited states, with excitation energies of 6.78 and 6.84 eV, belong to the antisymmetric irreducible representation B and are denoted as b_1 and b_2, respectively.

The transition dipole moments between the ground (g) state and the three excited states are depicted in Figure 1b: $\boldsymbol{\mu}_{ga}$ ($|\boldsymbol{\mu}_{ga}|$ = 0.77au) is parallel to the *Z* axis, and $\boldsymbol{\mu}_{gb_1}$ ($|\boldsymbol{\mu}_{gb_1}|$ = 1.95 au) and $\boldsymbol{\mu}_{gb_2}$ ($|\boldsymbol{\mu}_{gb_2}|$ = 1.29 au) are in the *XY* plane. (*P*)-2,2′-biphenol was assumed to be fixed on a surface by a (CH_2) chain free from the π electrons. The laboratory-fixed *Y* axis coincides with the single bond bridging the two phenol groups, and the rotation axis of the C_2 point group is placed along the laboratory-fixed *Z* axis parallel to the surface normal. The two phenol rings are twisted with respect to the *XY* plane by ±54.4° (i.e., 108.8°/2).

Let us first clarify the rotational behaviors of the π electrons of (*P*)-2,2′-biphenol just after excitation by linearly polarized UV laser pulses. To clarify the initial rotational dynamics, the time evolution of the π electrons was calculated using the time-dependent Schrödinger equation. We omitted the vibrational degrees of freedom under the fixed-nuclei condition. The effects of vibrations on the π-electron rotations were treated elsewhere.[10c] The electronic state at time *t* can be expressed in terms of the electronic state functions as $\Psi(t) = \sum_i c_i(t)\Phi_i \exp[-i\omega_i t]$, where Φ_i denotes the *i*th electronic wave function with angular frequency ω_i, which is an eigenfunction of the electronic Hamiltonian at the optimized geometry in the ground state. The time-dependent behavior of the electronic states can be obtained directly by solving the coupled equations of motion for $c_i(t)$ with the initial condition $c_g(0) = 1$; $c_i(0) = 0$ with $i \neq g$:

$$\frac{dc_\alpha(t)}{dt} = -\frac{i}{h}\sum_\beta c_\beta(t)V_{\alpha\beta}(t)\exp[-i(\omega_\beta - \omega_\alpha)t] \quad (1)$$

where $V_{\alpha\beta}(t)$ is the matrix element of the molecule−field interaction potential, $\hat{V}(t) = -\hat{\boldsymbol{\mu}}\cdot\mathbf{E}(t)$, where $\mathbf{E}(t)$ is the electric field of the laser and $\hat{\boldsymbol{\mu}}$ is the transition dipole moment operator. Since we are interested in ultrafast coherent π-electron rotations, the expectation value of the angular momentum at time *t* can be expressed as the sum of those originating from the two phenol rings:

$$\langle l(t)\rangle = \sum_{\alpha,\beta\neq g} \mathrm{Im}\, c_\beta^*(t)c_\alpha(t)\langle\Phi_\beta|(\hat{l}_{zL} + \hat{l}_{zR})|\Phi_\alpha\rangle \quad (2)$$

where α and β refer to the three excited states and $\hat{l}_{zK}$ is the operator for the *z* component of the electronic angular momentum, given by $\hat{l}_{zK} = -i\hbar\sum_j(x_{j,K}\partial/\partial y_{j,K} - y_{j,K}\partial/\partial x_{j,K})$, in which *j* represents the π electrons and K = L or R refers to the two phenol rings (see Figure 1b). The coordinates $x_{j,K}$ and $y_{j,K}$ are defined on phenol ring K, and the direction of the angular momentum vector $\mathbf{l}_{zK}$ is perpendicular to phenol ring K.

Figure 2 schematically shows the four patterns of π-electron rotations and the corresponding resultant angular momenta of

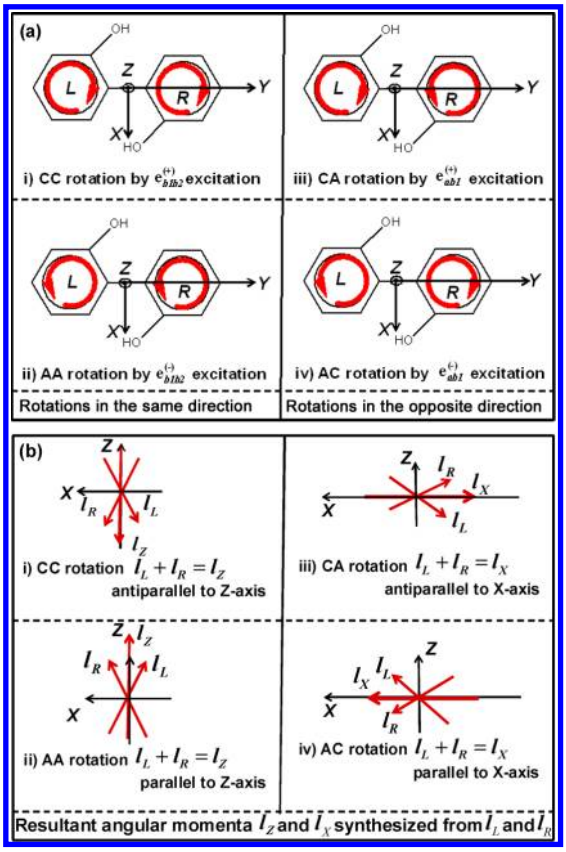

Figure 2. (a) Four patterns of π-electron rotation induced by selective coherent electronic excitations. For example, CA rotation means clockwise and anticlockwise rotations along the phenol rings L and R, respectively. (b) Resultant angular momenta $\mathbf{l}_Z$ and $\mathbf{l}_X$ for the four rotational patterns. $\mathbf{l}_L$ ($\mathbf{l}_R$) denotes the electron angular momentum of the L (R) ring.

(*P*)-2,2′-biphenol just after coherent excitations by selective linearly polarized UV pulses. These were calculated using eq 2. The polarization direction is expressed in terms of the unit vectors $\mathbf{e}^{(+)}_{\alpha,\beta}$ and $\mathbf{e}^{(-)}_{\alpha,\beta}$, with α, β = a, b_1, or b_2. Here, $\mathbf{e}^{(+)}_{\alpha,\beta}$ and $\mathbf{e}^{(-)}_{\alpha,\beta}$ are defined by $\mathbf{e}^{(+)}_{\alpha,\beta}\cdot\boldsymbol{\mu}_{g\alpha} = \mathbf{e}^{(+)}_{\alpha,\beta}\cdot\boldsymbol{\mu}_{g\beta}$ and $\mathbf{e}^{(-)}_{\alpha,\beta}\cdot\boldsymbol{\mu}_{g\alpha} = -\mathbf{e}^{(-)}_{\alpha,\beta}\cdot\boldsymbol{\mu}_{g\beta}$, respectively. Excitation by laser pulses with $\mathbf{e}^{(+)}_{\alpha,\beta}$ ($\mathbf{e}^{(-)}_{\alpha,\beta}$) polarization creates a linear combination of the two electronic

dx.doi.org/10.1021/ja3047848 | J. Am. Chem. Soc. XXXX, XXX, XXX−XXX

states α and β with an in-phase (out-of-phase) relationship; such excitation is hereafter called $\mathbf{e}^{(+)}_{\alpha,\beta}$ ($\mathbf{e}^{(-)}_{\alpha,\beta}$) excitation.

The schematic drawings on the left-hand side of Figure 2a represent the initial rotational directions of π electrons in the case in which a superposition of the two excited states b_1 and b_2, with the same irreducible representation of the point group C_2, is prepared. The upper (lower) drawing shows the rotational direction just after coherent $\mathbf{e}^{(+)}_{b_1b_2}$ ($\mathbf{e}^{(-)}_{b_1b_2}$) excitation, which leads to CC (AA) rotation, wherein the π electrons start to rotate along the two phenol rings in the same direction.

The left-hand side of Figure 2b shows the resultant angular momentum $\mathbf{l} = \mathbf{l}_L + \mathbf{l}_R$. The π-electron angular momentum $\mathbf{l}_L$ ($\mathbf{l}_R$) is perpendicular to the L (R) phenol ring, and the resultant total angular momentum (denoted as $\mathbf{l}_Z$) is parallel to the Z axis in the XZ plane. The directions of $\mathbf{l}_Z$ indicate that clockwise (anticlockwise) rotation around the Z axis is created by $\mathbf{e}^{(+)}_{\alpha,\beta}$ ($\mathbf{e}^{(-)}_{\alpha,\beta}$) excitation. The rotational directions agree with those expected from the time evolution of a coherently excited state $\Psi(t)$ consisting of two electronic states Φ_α and Φ_β that was prepared by a δ-function excitation: $\Psi(t) = c[\Phi_\alpha + \Phi_\beta \exp(-i\omega_{\beta\alpha}t)]$, where $\exp(-i\omega_{\beta\alpha}t)$ is the relative phase between the β and α states, in which $\omega_{\beta\alpha} > 0$ is the angular frequency difference between states α and β, and c is the normalization constant with the global phase. That is, the state after $\mathbf{e}^{(\pm)}_{\alpha,\beta}$ excitation evolves as $\Psi(0) = c(\Phi_\alpha \pm \Phi_\beta)$, $\Psi(T/4) = c(\Phi_\alpha \mp i\Phi_\beta)$, $\Psi(T/2) = c(\Phi_\alpha \mp \Phi_\beta)$, $\Psi(3T/4) = c(\Phi_\alpha \pm i\Phi_\beta)$, and $\Psi(T) = c(\Phi_\alpha \pm \Phi_\beta)$ for one cycle of oscillation of the coherent state. Here, the upper (lower) sign corresponds to $\mathbf{e}^{(+)}_{\alpha,\beta}$ ($\mathbf{e}^{(-)}_{\alpha,\beta}$) excitation, and T denotes the oscillation period, given by $T \equiv 2\pi/\omega_{\beta\alpha}$. At $t = T/4$ and $3T/4$, the absolute magnitude of the angular momentum becomes maximum.

The schematic drawings on the right-hand side of Figure 2a,b represent π-electron rotations and the resultant angular momenta in the case in which a superposition of the two excited states a and b_1 with different irreducible representations is prepared. The π electrons start to rotate along the two phenol rings in opposite directions (CA or AC rotation). Therefore, the total angular momentum parallel to the Z axis is zero, and the nonzero resultant angular momentum (denoted as $\mathbf{l}_X$) is generated along the X axis in the XZ plane. If the two phenol rings are in the same plane (i.e., in biphenol without a twist), both $\mathbf{l}_X$ and $\mathbf{l}_Z$ vanish. Furthermore, the simulation results indicate that $\mathbf{e}^{(+)}_{ab_1}$ and $\mathbf{e}^{(-)}_{ab_1}$ excitations induce CA and AC rotations, respectively. The directions of the π-electron rotations are the same as those expected from the time evolution of the coherent state as well. However, it should be noted that the induced rotational directions are incidental because the coherent states created by $\mathbf{e}^{(+)}_{ab_1}$ and $\mathbf{e}^{(-)}_{ab_1}$ excitations are not eigenfunctions of the electronic angular momentum operator around the X axis but instead are eigenfunctions of that around the Z axis. The rotational direction depends on the coherently excited electronic state. In fact, for a coherent state involving the two excited states a and b_2, the directions of $\mathbf{l}_X$ created by $\mathbf{e}^{(+)}_{ab_2}$ and $\mathbf{e}^{(-)}_{ab_2}$ excitations are opposite to those expected from the time evolution of the system. Detailed explanations will be given elsewhere.

So far, (*P*)-2,2′-biphenol has been treated. For another type of enantiomer, (*M*)-2,2′-biphenol, the rotational directions of the π electrons can be obtained by changing the signs of the corresponding rotational directions of (*P*)-2,2′-biphenol. For a racemic mixture, electron rotation cannot be observed.

Let us now consider quantum control of π-electron rotations for two-dimensional current switching on the basis of the results shown in Figure 2. Here, two-dimensional switching means a sequential variation of the electronic angular momentum with its definite sign (plus or minus) along the Z or X axis. We note that switching should be carried out before reverse rotation of the π electrons begins, since the prepared coherent states are not eigenstates. For this purpose, we tested a sequential four-step control expressed as $\mathbf{l}_Z(-) \rightarrow \mathbf{l}_X(+) \rightarrow \mathbf{l}_Z(+) \rightarrow \mathbf{l}_X(-)$, corresponding to the switching of rotational patterns CC → AC → AA → CA. Here, $\mathbf{l}_Z(-)$ ($\mathbf{l}_X(+)$) denotes the π-electron angular momentum along the Z (X) axis with a negative (positive) sign [i.e., clockwise (anticlockwise) rotation of the π electrons around the corresponding axis].

Figure 3a shows a three-dimensional plot of the resultant angular momentum switching based on the sequential four-step

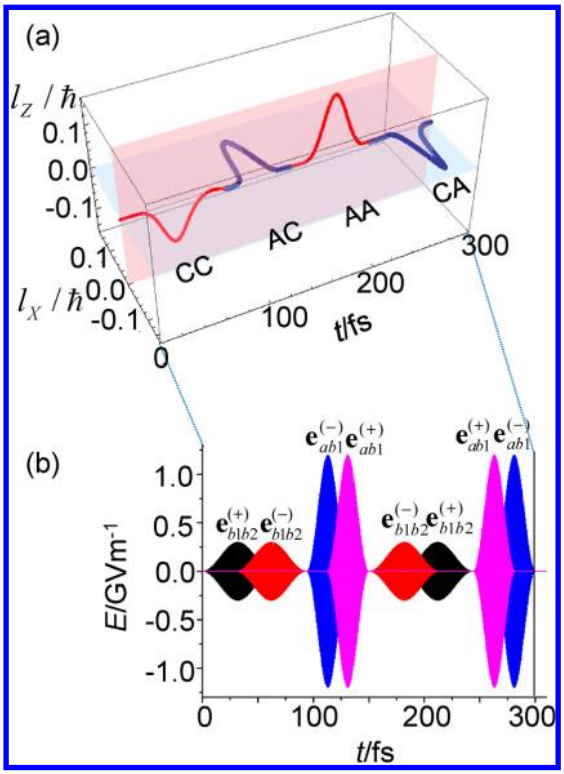

Figure 3. (a) Sequential four-step switching of π-electron rotations in (*P*)-2,2′-biphenol. (b) Electric fields of the sequence of overlapped pump and dump pulses.

scheme. It can be seen from Figure 3a that the π-electron rotations were successfully controlled by the pulses depicted in Figure 3b. That is, both the rotational axis (parallel to the Z or X axis) and the rotational direction around the axis (clockwise or anticlockwise) were satisfactorily controlled by the sequential four-step process. In Figure 3b, the control at each switching step was carried out by using pump and dump pulses with specific polarization directions. A pulsed laser with an amplitude of 1.2 GV/m (=1.9×10^{11} W/cm^2)[14] was used in the second and fourth steps. The Stark shift was on the order of 0.01 eV (see the SI). This allowed us to omit the Stark effects in Figure 3a.

The pulses shown in Figure 3b have two features: first, the pump (dump) pulse for each step has $\mathbf{e}^{(+)}_{\alpha,\beta}$ ($\mathbf{e}^{(-)}_{\alpha,\beta}$) or $\mathbf{e}^{(-)}_{\alpha,\beta}$ ($\mathbf{e}^{(+)}_{\alpha,\beta}$) polarization. Each pulse has an energy width that is sufficient for coherent excitation of two quasi-degenerate electronic

dx.doi.org/10.1021/ja3047848 | J. Am. Chem. Soc. XXXX, XXX, XXX−XXX

excited states, as shown in Figure 1. Second, the pump and dump pulses partially overlap. For the first step (i.e., creation of CC rotation), for example, the electric field of the pump pulse was $\mathbf{E}^{(+)}_{b_1b_2}(t) = \mathbf{e}^{(+)}_{b_1b_2}\mathbf{E}^{0}_{b_1b_2} \sin^2(\pi t/T_{b_1b_2}) \sin(\omega_{c,b_1b_2}t)$, while that of the dump pulse was $\mathbf{E}^{(-)}_{b_1b_2}(t) = \mathbf{e}^{(-)}_{b_1b_2}\mathbf{E}^{0}_{b_1b_2} \sin^2[\pi(t - t^{pd}_{b_1b_2})/T_{b_1b_2}] \sin(\omega_{c,b_1b_2}t + \pi/2)$, where $\mathbf{E}^{0}_{b_1b_2}$ is the amplitude of the pulse, $T_{b_1b_2}$ (here equal to 60.9 fs) is the oscillation period between the two excited states b_1 and b_2, ω_{c,b_1b_2} is the central frequency between the two excited states, and $t^{pd}_{b_1b_2}$ is the time interval between the pump and dump pulses, which was set to $T_{b_1b_2}/2$ (see the SI). The angle between the two polarization directions $\mathbf{e}^{(+)}_{b_1b_2}$ and $\mathbf{e}^{(-)}_{b_1b_2}$ was 113.5°.

For the present ultrafast quantum switching, overlap between the pump and dump pulses is essential: the resultant electric field is rotated as an elliptically polarized one in the overlapped region, and the electric field forces the rotating π electrons to induce the reverse rotation that occurs in this region. As a result, the electronic angular momentum of the π electrons is erased (see the SI).

In the present treatment, the effects of couplings between the π electrons and vibrations were omitted under the fixed-nuclei condition since in the sequential switching scheme, the target molecule returns to the ground state after each switching process, which occurs within an ultrashort time (~60 fs). Electron−vibration couplings induce dephasings in electron rotations,[10c] and for a quantitative discussion, these couplings have to be taken into account.[15] The torsional mode between the two rings can be expected to have a significant influence on the control of the angular momentum.[16]

Finally, it would be fascinating to explore a method for measuring the coherent electronic dynamics of a nonplanar chiral aromatic molecule. In principle, angular momentum can be examined by detecting ring currents.[9]

In conclusion, we have theoretically clarified how the four π-electron rotational patterns of a nonplanar chiral aromatic molecule, (*P*)-2,2′-biphenol, can be prepared using linearly polarized UV pulses. We have found two key factors for determining the rotational patterns. The first key factor is the symmetry of the coherent electronic states. That is, π electrons in the two phenol rings begin to rotate in the same direction (CC or AA rotation) when quasi-degenerate states with the same irreducible representation are coherently excited. When two excited states with different irreducible representations are coherently excited, on the other hand, the rotational directions in the two phenol rings are opposite (CA or AC rotation). The second key factor is the relative phase between the two coherently excited states. CC rotation, for example, can be prepared by an in-phase coherent excitation, while AA rotation can be prepared by an out-of-phase coherent excitation. Moreover, we have demonstrated simple two-dimensional switching in 2,2′-biphenol using a sequence of overlapped pump and dump pulses with a selected relative phase between the two pulses and their polarization directions. From recent rapid progress in the generation of ultrashort (attosecond) pulses, it is expected that quantum switching of electronic currents can be realized.[17−19]

■ ASSOCIATED CONTENT

Ⓢ Supporting Information

Results of quantum-chemical calculations, procedures used for the pump−dump pulse control, and complete ref 12 (as ref S1). This material is available free of charge via the Internet at http://pubs.acs.org.

■ AUTHOR INFORMATION

Corresponding Author

fujimurayuichi@m.tohoku.ac.jp

Notes

The authors declare no competing financial interest.

■ ACKNOWLEDGMENTS

This work was supported in part by JSPS (Research Grant 23550003). Y.F. thanks the National Science Council of Taiwan for financial support. We are grateful to Prof. H. Nakamura for his critical comments. H.M. thanks Prof. S. D. Chao for his encouragement.

■ REFERENCES

(1) Krause, P.; Klamroth, T.; Saalfrank, P. *J. Chem. Phys.* **2005**, *123*, No. 074105.

(2) Král, P.; Seideman, T. *J. Chem. Phys.* **2005**, *123*, No. 184702.

(3) Wei, J. J.; Schafmeister, C.; Bird, G.; Paul, A.; Naaman, R.; Waldeck, D. H. *J. Phys. Chem. B* **2006**, *110*, 130.

(4) Fujimura, Y.; Sakai, H. *Electronic and Nuclear Dynamics in Molecular Systems*; World Scientific: Singapore, 2011; p 11.

(5) Anthony, J. E. *Chem. Rev.* **2006**, *106*, 5028.

(6) Bonifas, A. D.; McCreery, R. L. *Nat. Nanotechnol.* **2010**, *5*, 612.

(7) Streitwieser, A., Jr. *Molecular Orbital Theory for Organic Chemists*; Wiley: New York, 1961; p 117.

(8) Ulusoy, I.; Nest, M. *J. Am. Chem. Chem. Soc.* **2011**, *133*, 20230.

(9) (a) Barth, I.; Manz, J.; Shigeta, Y.; Yagi, K. *J. Am. Chem. Soc.* **2006**, *128*, 7043. (b) Barth, I.; Manz, J. *Angew. Chem.* **2006**, *118*, 3028; *Angew. Chem., Int. Ed.* **2006**, *45*, 2962. (c) Barth, I.; Manz, J. In *Progress in Ultrafast Intense Laser Science VI*; Springer Series in Chemical Physics, Vol. *99*; Springer: Berlin, 2010; p 21.

(10) (a) Kanno, M.; Kono, H.; Fujimura, Y. *Angew. Chem., Int. Ed.* **2006**, *45*, 7995. (b) Kanno, M.; Hoki, K.; Kono, H.; Fujimura, Y. *J. Chem. Phys.* **2007**, *127*, No. 204314. (c) Kanno, M.; Kono, H.; Fujimura, Y.; Lin, S. H. *Phys. Rev. Lett.* **2010**, *104*, No. 108302.

(11) Wolf, C. *Dynamic Stereochemistry of Chiral Compounds: Principles and Applications*; RSC Publishing: Cambridge, U.K., 2008; p 6.

(12) Frisch, M. J.; et al. *Gaussian 09*, revision E.01; Gaussian, Inc.: Wallingford, CT, 2009.

(13) Jacquemin, D.; Wathelet, V.; Perpète, E. A.; Adamo, C. *J. Chem. Theory Comput.* **2009**, *5*, 2420.

(14) The atomic unit of intensity is 3.51×10^{16} W/cm^2, which corresponds to $E = 5.14$ GV/cm.

(15) Moore, K.; Rabitz, H. *Nat. Chem.* **2012**, *4*, 72.

(16) Parker, S. M.; Ratner, M. A.; Seideman, T. *J. Chem. Phys.* **2011**, *135*, No. 224301.

(17) Yuan, K.-J.; Bandrauk, A. D. *J. Phys. B: At., Mol. Opt. Phys.* **2012**, *45*, No. 074001.

(18) Goulielmakis, E.; Loh, Z.-H.; Wirth, A.; Santra, R.; Rohringer, N.; Yakovlev, V. S.; Zherebtsov, S.; Pfeifer, T.; Azzeer, A. M.; Kling, M. F.; Leone, S. R.; Krausz, F. *Nature* **2010**, *466*, 739.

(19) Chen, S.; Gilbertson, S.; Wang, H.; Chini, M.; Zhao, K.; Khan, S. D.; Wu, Y.; Chang, Z. *Adv. Multi-Photon Processes Spectrosc.* **2011**, *20*, 127.